AME 408 Final Project Report

Centrifugal Governor

December 4th, 2025

AME 408

Professor Babak Boloury

Group 1

Google Drive Folder Link: AME 408 Final Project

Christopher Heald

Charles Hernandez

Lucas Rival

Alessandro Tasso

Summary and Methodology:

The part was created based on the provided drawings (shown below for quick reference) and initially left dimensionless. The dimensions were then applied based on the design criteria using global variables for ease of access without creating large numbers of configurations.

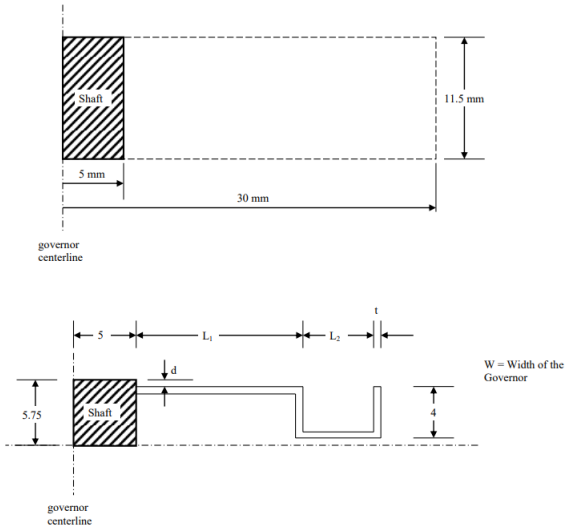

Figure 1: Copy of provided drawing for easy reference. Sourced from USC AME-408 Fall 2026 final project document.

Equations between dimensions allowed the input numbers to accurately change the model to the correct configuration. The MIRAGE 250 CVM material was created as a custom material with the given material properties and applied to the model, as shown in image below.

Modulus of Elasticity	E = 205 GPa
Poisson's Ratio	$\nu = 0.3$
Mass Density	$\rho = 7850\ kg/m^3$
Maximum Allowable Stress	$\sigma_a = \sigma_{VM} = 1750$ MPa

Figure 2: Image of MIRAGE 250 CVM material properties for easy reference. Sourced from USC AME-408 Fall 2026 final project document.

The model contains three planes of symmetry, and as such was cut so that only 1/8 of the model remained. Then, a static structural and frequency study were created. Utilizing the "On Flat Faces" fixture, a constraint in the normal direction was placed on the two planes of symmetry that intersected the model. An external centrifugal load of 6,000 rad/s was placed on the central axis of the model, and the initial mesh size was chosen to be 0.6mm.

Following the design criteria, a spreadsheet was used for tracking configurations. Formulas were created to show go/no-go indications for the inter-dimensional relations between L1 and L2; all dimensions were kept being multiples of 0.25mm, and the rest of the criteria were implemented and tracked as given. The container fitment criteria was achieved through ensuring that axial deflection did not break the plane of the top face of the shaft and through ensuring that the overall length combined with thickness and the 5mm shaft diameter did not exceed 24.75mm, leaving a 0.25mm fitment tolerance based on the allowable sizing increment of 0.25mm (the governor was undersized to ensure its nominal dimension was not the same as the inner diameter of the housing). The process of narrowing down the possible permutations of dimensional combinations began with the stated criteria to maximize width above length and thickness. This led to a fixed 6.75mm (about 0.27 in) width being used for all configurations as this was the largest width which did not result in interference between the individual governor arms and their fillets (fillets were applied to the maximum radius of curvature allowed based on the design criteria and instructions to not allow the maximum Von Mises stress to be where the arms connect to the shaft). Following this, it was proved through large-scale trend analysis about dimensional changes that increased thickness resulted in lower model stress, lower deflection, and higher fundamental frequency. When combined with the design intent to maximize the overall length (sum of L1 and L2) while minimizing thickness as a secondary concern, a more methodical strategy for predesignating testable permutations was developed as follows:

1) Thickness was fixed in 0.25mm increments between 1 and 1.5mm based on trends observed during initial trend analysis
2) L1 was varied in whole number increments
3) For each increment of L1, the upper and lower bounds of the range of L2 values which satisfied the relationship between the two as well as the container fitment requirement were determined
4) All permutations of L2 for the given L1 were listed in 0.25mm increments
5) This was repeated for each increment of L1 until either there ceased to be a combination of L1 and L2 which satisfied the two requirements or until the sum of L1 and L2 and material thickness dropped below 20mm
6) Thickness was cycled to the next increment, and the process was repeated

Once a table of testable permutations had been developed, the upper and lower bounds of each L1/thickness combination were analyzed in SolidWorks FEA software based on the given design criteria. This method quickly highlighted dimensional regions of interest while eliminating groups of permutations which did not meet design criteria. As a note, trend analysis had previously shown the dimension labelled as “d” in the provided drawings to have minimal impact on frequency, stress, and deflection however it was clearly relevant to ensuring that axial deflection did not exceed available container space. As such, it was not considered relevant to the study and was held at 1 for initial trials as this was the larger of the two possible midpoint options in the set of possible values {0, 0.25, 0.5, 0.75, 1, 1.25, 1.5, 1.75} between the values

which resulted in the governor arm becoming flush with either the governor centerline (x-axis in drawings provided) or with the flat face of the shaft. It is worth noting also that given the deflection requirement being less than 1.15mm of axial deflection, a more reasonable approach would have been to set the variable *d* equal to 1.25mm as this would ensure that if the deflection condition was met, so too was the container space requirement so long as overall governor diameter did not exceed 24.75mm.

t (mm)	L1 (mm)	L2 (mm)	W (mm)	d (mm)	<= L1 <= 1+L2+t<25m		SUM	Ratio	Length
1.25	15.25	8.5	6.75	1	YES	NO	25	1.794118	23.75
1.25	15.25	8.25	6.75	1	NO	YES	24.75	1.848485	23.5
1.25	15	8.75	6.75	1.25	YES	NO	25	1.714286	23.75
1.25	15	8.5	6.75	1.25	YES	YES	24.75	1.764706	23.5
1.25	15	8.25	6.75	1.25	NO	YES	24.5	1.818182	23.25
1.25	14.75	9	6.75	1.25	YES	NO	25	1.638889	23.75
1.25	14.75	8.75	6.75	1.25	YES	YES	24.75	1.685714	23.5
1.25	14.75	8.5	6.75	1.25	YES	YES	24.5	1.735294	23.25
1.25	14.75	8.25	6.75	1.25	YES	YES	24.25	1.787879	23
1.25	14.75	8	6.75	1.25	NO	YES	24	1.84375	22.75
1.25	14.5	9.25	6.75	1.25	YES	NO	25	1.567568	23.75
1.25	14.5	9	6.75	1.25	YES	YES	24.75	1.611111	23.5
1.25	14.5	8.75	6.75	1.25	YES	YES	24.5	1.657143	23.25
1.25	14.5	8.25	6.75	1.25	YES	YES	24	1.757576	22.75
1.25	14.5	8	6.75	1.25	NO	YES	23.75	1.8125	22.5
1.25	14.25	9.5	6.75	1.25	YES	NO	25	1.5	23.75
1.25	14.25	9.25	6.75	1.25	YES	YES	24.75	1.540541	23.5
1.25	14.25	9	6.75	1.25	YES	YES	24.5	1.583333	23.25
1.25	14.25	8.75	6.75	1.25	YES	YES	24.25	1.628571	23
1.25	14.25	8.5	6.75	1.25	YES	YES	24	1.676471	22.75
1.25	14.25	8.25	6.75	1.25	YES	YES	23.75	1.727273	22.5
1.25	14.25	8	6.75	1.25	YES	YES	23.5	1.78125	22.25
1.25	14.25	7.75	6.75	1.25	NO	YES	23.25	1.83871	22

Score	t (mm)	L1 (mm)	L2 (mm)	W (mm)	d (mm)	<= L1 <= 1+L2+t<25m		SUM	Ratio	Length
97.17262	1.5	15.25	8.25	6.75	1	NO	NO	25	1.848485	23.5
96.87262	1.5	15.25	8	6.75	1	NO	YES	24.75	1.90625	23.25
98.07262	1.5	15.5	8.75	6.75	1	YES	NO	25.75	1.771429	24.25
97.77262	1.5	15.5	8.5	6.75	1	NO	NO	25.5	1.823529	24
96.87262	1.5	15.5	7.75	6.75	1	NO	YES	24.75	2	23.25
97.17262	1.5	14.75	8.75	6.75	1	YES	NO	25	1.685714	23.5
96.87262	1.5	14.75	8.5	6.75	1	YES	YES	24.75	1.735294	23.25
96.57262	1.5	14.75	8.25	6.75	1	YES	YES	24.5	1.787879	23
96.27262	1.5	14.75	8	6.75	1	NO	YES	24.25	1.84375	22.75
97.17262	1.5	14.5	9	6.75	1	YES	NO	25	1.611111	23.5
96.87262	1.5	14.5	8.75	6.75	1	YES	YES	24.75	1.657143	23.25
96.57262	1.5	14.5	8.5	6.75	1	YES	YES	24.5	1.705882	23
96.27262	1.5	14.5	8.25	6.75	1	YES	YES	24.25	1.757576	22.75
95.97262	1.5	14.5	8	6.75	1	NO	YES	24	1.8125	22.5
97.17262	1.5	14.25	9.25	6.75	1	YES	NO	25	1.540541	23.5
96.87262	1.5	14.25	9	6.75	1	YES	YES	24.75	1.583333	23.25
96.27262	1.5	14.25	8.5	6.75	1	YES	YES	24.25	1.676471	22.75
95.67262	1.5	14.25	8	6.75	1	YES	YES	23.75	1.78125	22.25
95.37262	1.5	14.25	7.75	6.75	1	NO	YES	23.5	1.83871	22
95.97262	1.5	14.25	8.25	6.75	1.25	YES	YES	24	1.727273	22.5
96.27262	1.5	14.5	8.25	6.75	1.25	YES	YES	24.25	1.757576	22.75

Figure 3: Representative image of dimensional permutation table for 1.25 and 1.5mm thickness respectively (left to right). Note the "SUM" column used to ensure governor size did not exceed container diameter, the "Length" column used to optimize possible L1/L2 combinations, and the colored go/no-go indication used to illustrate the upper/lower bounds of testable regions.

As testing progressed it became apparent that the design would be optimized at a thickness of 1.25 or 1.5mm with a L1/L2/thickness sum as closed to 24.75 as possible and an L1/L2 sum as close to 23.25 or 23.5 as possible (for 1.5 and 1.25mm respectively based on 24.75 minus material thickness). The results of the study are contained in the following section. For testing, a single mesh size of 0.6mm was used for initial testing based on the findings of the earlier trend analysis. This mesh size was consistently found to be adequate for characterization of the part early in the testing process and allowed permutations which violated the design criteria to be removed without extensive testing. Further mesh refinements had a negligible impact on calculated modal and deflection values. The only major problems encountered during this study stemmed from issues with the dimension variables and their application. Once this was accomplished, the process was smooth.

Analysis

When creating the part, two different configurations were used: one with fillets and one without. For the fillets, they are not a standard size across the body. Two fillet sizes were used based on the provided directions. For the first fillet on the arm connecting to the center shaft, the radius of curvature was set to 0.2mm as shown below.

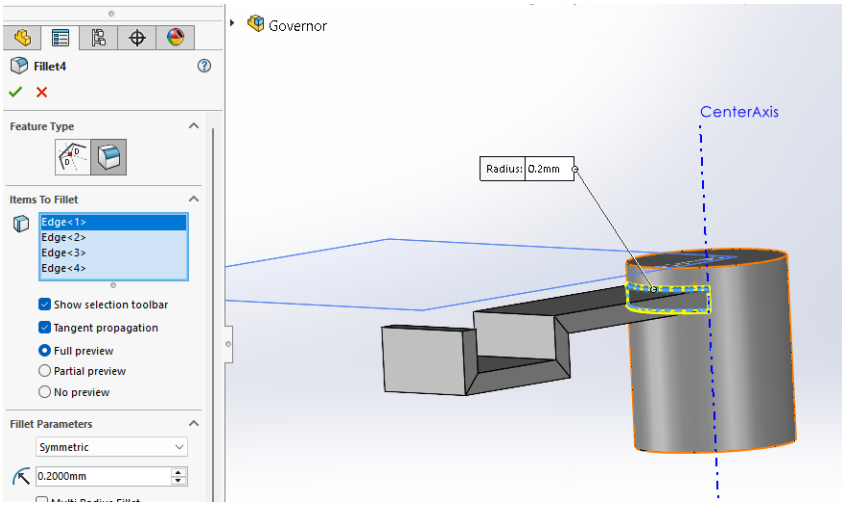

Figure 4: 0.3mm fillet at arm/shaft junction.

A second fillet was added to L1, with a radius of 0.3mm on all the outer edges of the arm. This fillet also connects at the center with the shaft, interacting with the previous fillet, shown below.

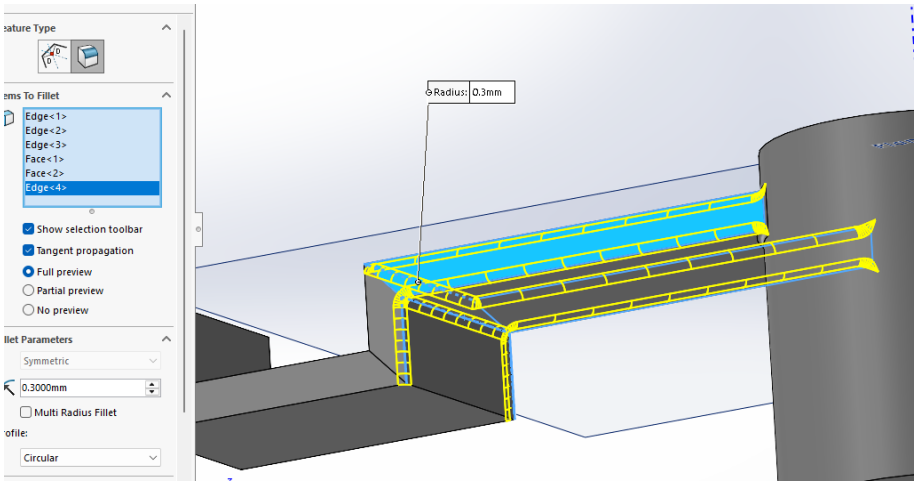

Figure 5: Representative image of first 0.3mm fillet.

An additional fillet of 0.3mm was placed on the bottom face and top face at the end of the arm. This fillet is self-contained and does not touch the other fillets, as shown below.

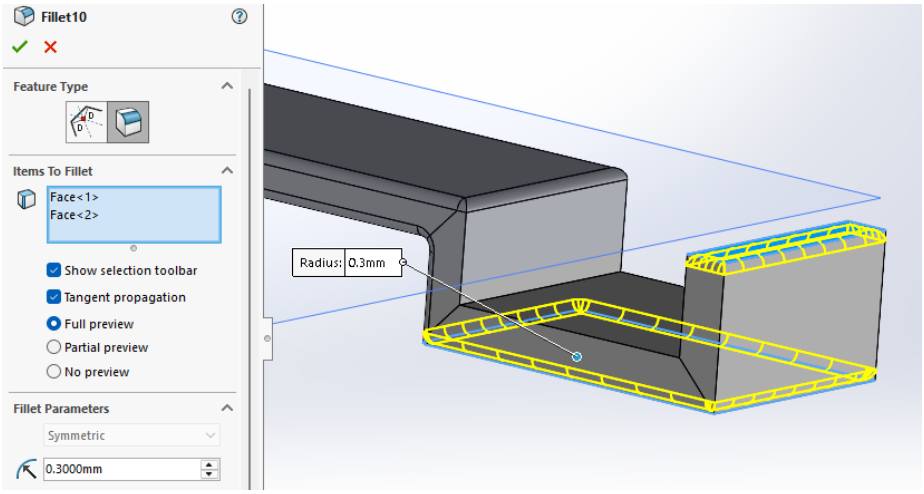

Figure 6: Representative image of the second 0.3mm fillet.

One design requirement was to utilize fillets to move stress concentrations away from the leg/shaft junction. This was achieved and is demonstrated in the images below.

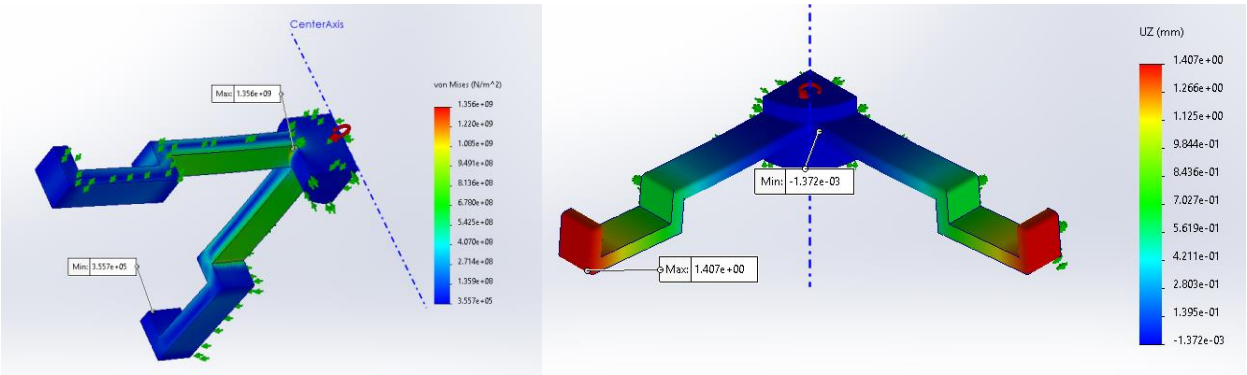

Figure 6: Maximum Von Mises stress for shaft/arm intersection fillet (0.2mm, filleted part shown on bottom)

It is worth noting that while the instructions called for fillets to only be used for structural benefit, the edge break fillet used along the outside edges of the arms does not reduce stress. This was an upstream misinterpretation that was caught too late in the process to reverse. It should instead have only been applied to the edges parallel to the one that holds the maximum stress value shown in the image below, resulting in a smooth transfer of internal forces with no singularity. While the edge break was not structurally necessary, it is a common manufacturing technique to reduce sharp edges and boundary imperfections and has no major impact on the analysis other than potentially increasing mesh complexity. However, it must be noted that the addition of fillets on the arm/shaft intersection and the arms themselves successfully moved the maximum Von Mises stress from where legs connect to the shaft to the first filleted corner of the arm itself, as shown in the diagram below.

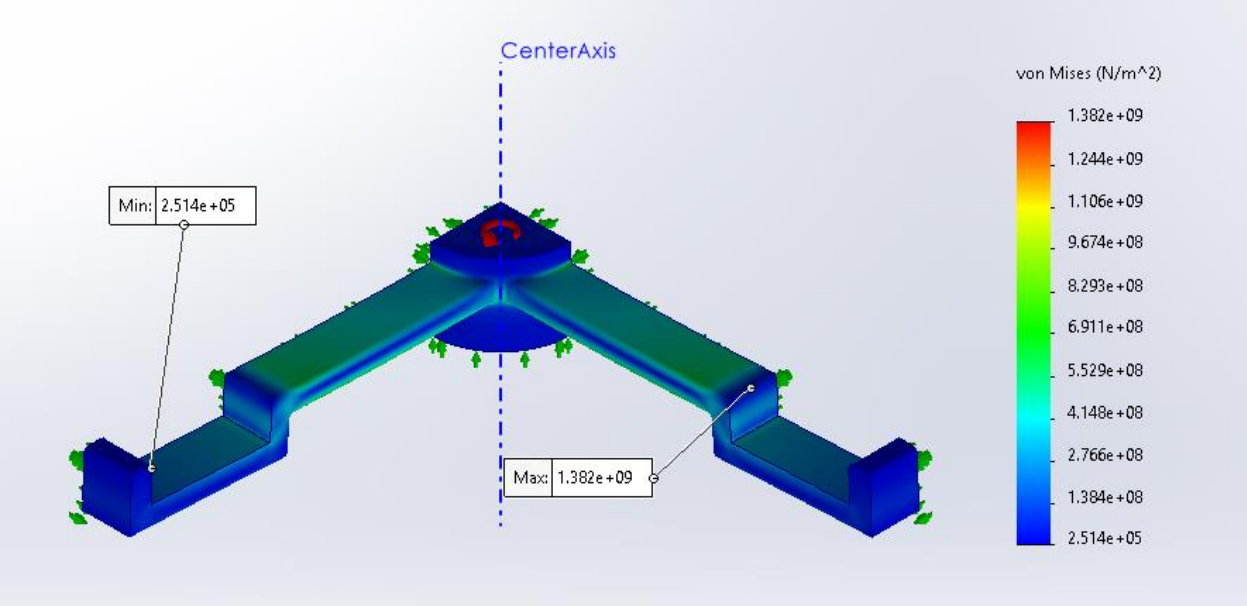

Figure 7: New maximum Von Mises stress location after 0.2mm and 0.3mm fillets

To run static and frequency testing on the modeled part, the part was cut along three planes: the front plane, right plane, and the top plane. With the part being symmetric around these three planes, reduction of computing intensity and computations allow for finer meshes and more accurate simulations.

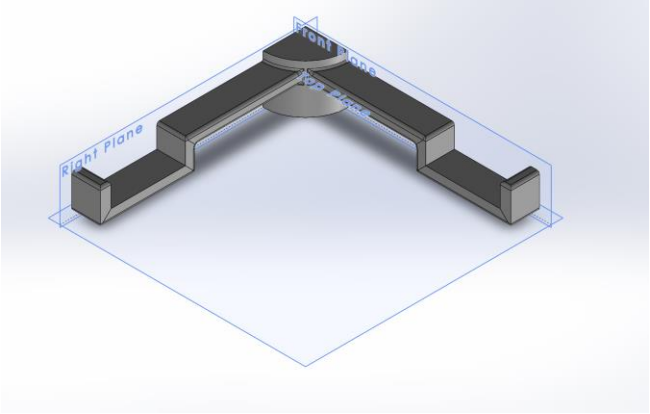

Figure 8: Part simplification cuts.

A static simulation was created to test the axial stress created from the centrifugal force. However, to simulate the entire governor rather than the cut part being tested, different conditions needed to be applied to recreate the entirety of the part as well as correct boundaries and forces to simulate the forces the part would experience during its use. Firstly, a fixture was placed on the flat surfaces at which the part was cut due to symmetry. This fixture was applied normally to the surface inward.

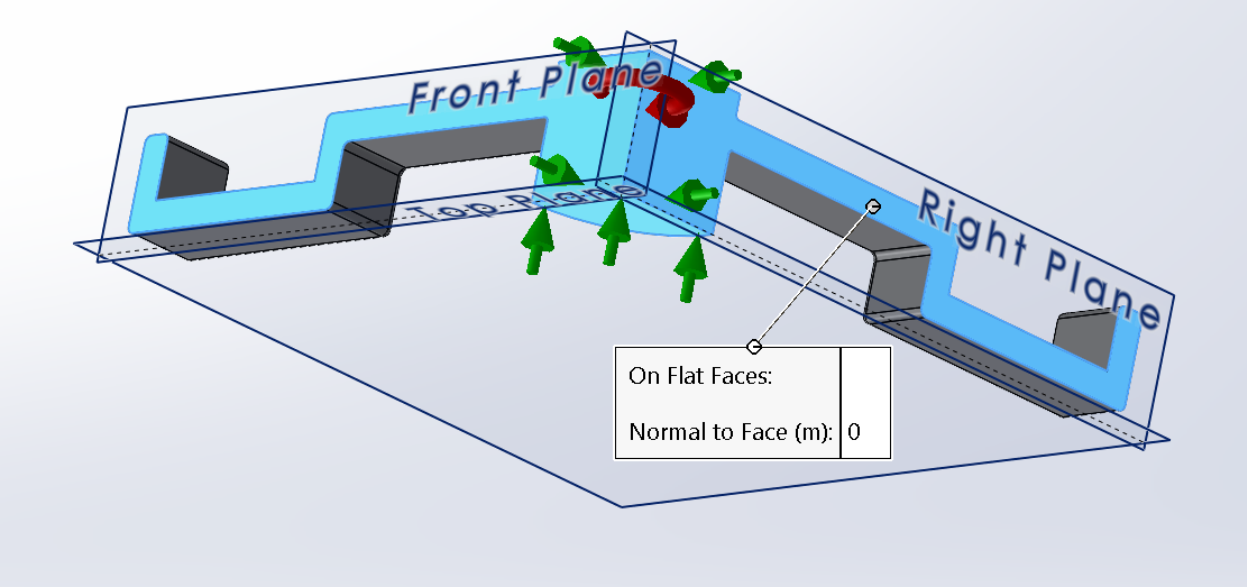

Figure 8: Shaft fixturing for static structural analysis.

With the part now constrained with boundary conditions simulating the entirety of the part, a centrifugal force was placed at the shaft. The axis of rotation is about the axis labelled CenterAxis in the image below, with a value of 6000 rad/s in the counterclockwise direction.

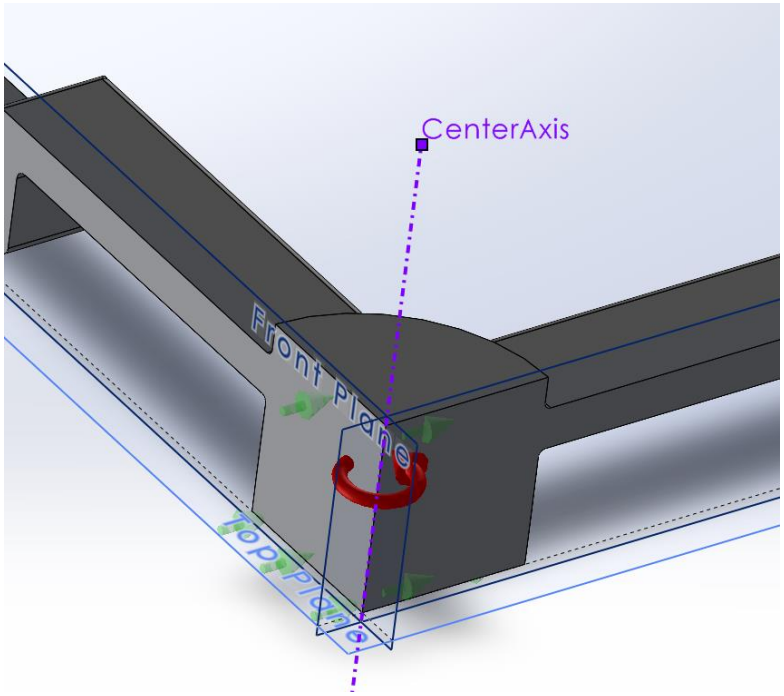

Figure 9: Part loading boundary condition

A frequency study was created to see the natural frequencies and their amplitudes. Similarly to the static study, the axes of symmetry were used to cut the part to perform testing.

Simulating the entire part came in the form of adding fixtures on the flat surfaces where the part was cut normal to the surface.

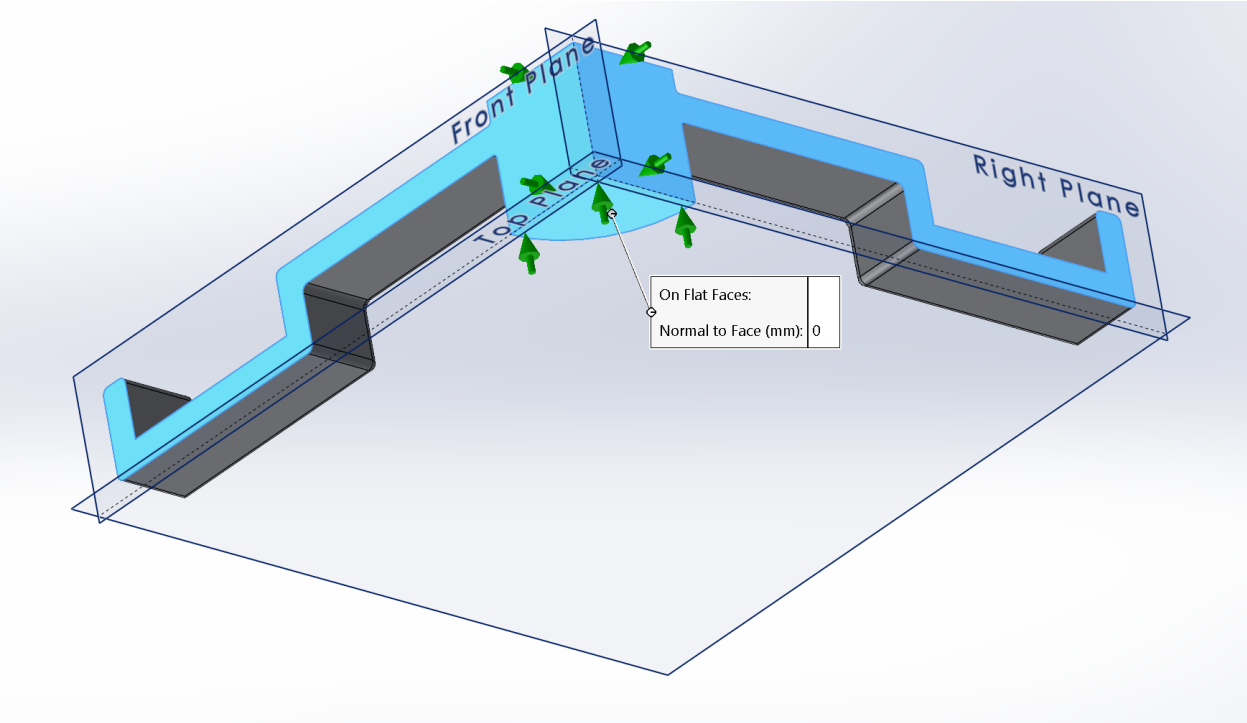

Figure 10: Shaft fixturing for modal analysis.

Results

Through the methods described above, the optimal governor dimensions for the constraints provided in the problem were narrowed down to the final values reported in the table below.

Score	t (mm)	L1 (mm)	L2 (mm)	W (mm)	d (mm)
96.872619	1.5	14.75	8.5	6.75	1.5
1.4*L2 <= L1 <= 1.8*L2?	L1+L2+t<25mm?	<2000Hz?	<1.15mm?	In Container?	Fillets?
YES	YES	YES	YES	YES	YES
Total Length	δ_total (mm)	f1 (Hz)	δ_axial (mm)	Mass (g)	σ_max (MPa)
24.75	0.9324	1567.6	0.9196	3.266842	1421

Figure 11: Optimal governor dimensions displayed alongside go/no-go conditions that verify all required constraints are met, and final mesh results. The "Score" is a weighted average of 50 percent width, 30 percent length, and 20 percent thickness which was solely used during trend analysis as a potential metric for grouping similar configurations.

Once the final dimensions were chosen based on the initial mesh results, a convergence study was completed to ensure accuracy of the results. The first mesh used was very coarse and for each following simulation the mesh size was reduced by ½, until the error reduced to under 5% for the problem. All required values converged well under 1% convergence error except for the maximum stress which only converged to 2.74%. The mesh would have been further refined to minimize this max stress error; however, computing power became the limiting factor with the final simulation taking more than half an hour to run at the final mesh sizes. Results from two convergence studies are outlined in the tables below and explained further in the following paragraph.

Mesh Size (mm)	δ_axial (mm)	PE %	σ_max (MPa)	PE %	deformation (mm)	PE %	f1 (Hz)	PE %	Mass (g)	PE %
3	0.9184	"----------"	1241	"----------"	0.9311	"----------"	1573.9	"----------"	3.266842	"--------"
1.5	0.9198	0.152207002	1354	8.345642541	0.9325	0.150134048	1571.1	0.178219082	3.266842	0
0.75	0.92	0.02173913	1447	6.427090532	0.9328	0.032161235	1570.3	0.050945679	3.266842	0
0.6	0.9201	0.010868384	1346	7.50371471	0.9326	0.021445421	1568.7	0.101995283	3.266842	0
0.5	0.9198	0.021743857	1365	6.007326007	0.9327	0.010721561	1568.6	0.108376897	3.266842	0
0.375	0.9197	0.010873111	1382	1.230101302	0.9325	0.021447721	1569.7	0.070077085	3.266842	0
0.1875	0.9196	0.010874293	1421	2.744546094	0.9324	0.010725011	1567.6	0.133962746	3.266842	0

Figure 12: Convergence table with final length, width, and thickness values for d=1.5

Mesh Size (mm)	δ_axial (mm)	PE %	σ_max (MPa)	PE %2	deformation (mm)	PE %3	f1 (Hz)	PE %4	Mass (g)	PE %5
3	0.9012	"----------"	966	"----------"	0.9135	"----------"	1594.7	"----------"	3.26684204	"----------"
1.5	0.92	2.043478261	1333	27.53188297	0.9326	2.048037744	1569.8	1.586189323	3.26684204	0
0.6	0.9186	0.152405835	1266	5.292259084	0.9312	0.150343643	1571	0.076384468	3.26684204	0
0.5	0.9195	0.097879282	1325	4.452830189	0.9322	0.107273117	1568.4	0.165774037	3.26684204	0
0.375	0.9242	0.508547933	1380	3.985507246	0.9368	0.491033305	1557.4	0.706305381	3.26684204	0
0.25	0.9195	0.511147363	1393	0.933237617	0.9323	0.48267725	1568	0.676020408	3.26684204	0
0.125	0.9196	0.010874293	1452	4.063360882	0.9324	0.010725011	1569	0.063734863	3.26684204	0

Figure 13: Convergence table with final length, width, and thickness values for d=1.25

Figure 12 shows the final, optimal configuration however the impact of the distance between the top face of the governor arms and the top flat face of the shaft, dimension *d*, is shown by a similar analysis run for an otherwise identical configuration with a change to this dimension shows a minimal, but not statistically significant, increase to maximum Von Mises stress. The final configuration was chosen based on this decrease as the major observed impact of changes to *d* was the ability to move the arm down the shaft to ensure its deflection does not result in interference with container walls.

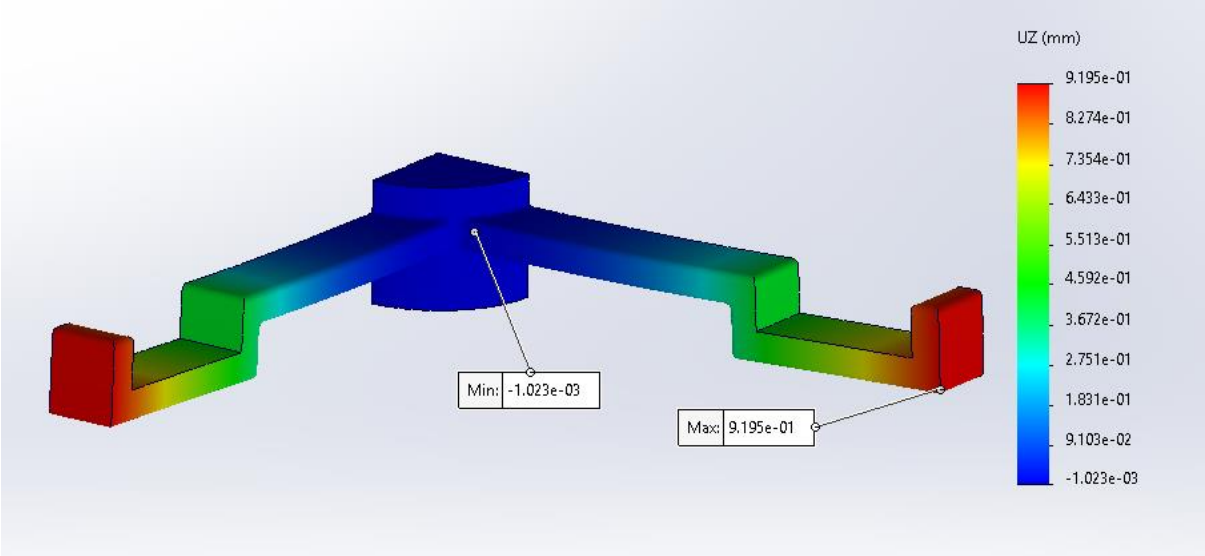

Figure 14: Axial displacement plot, Mesh Size: 0.1875mm

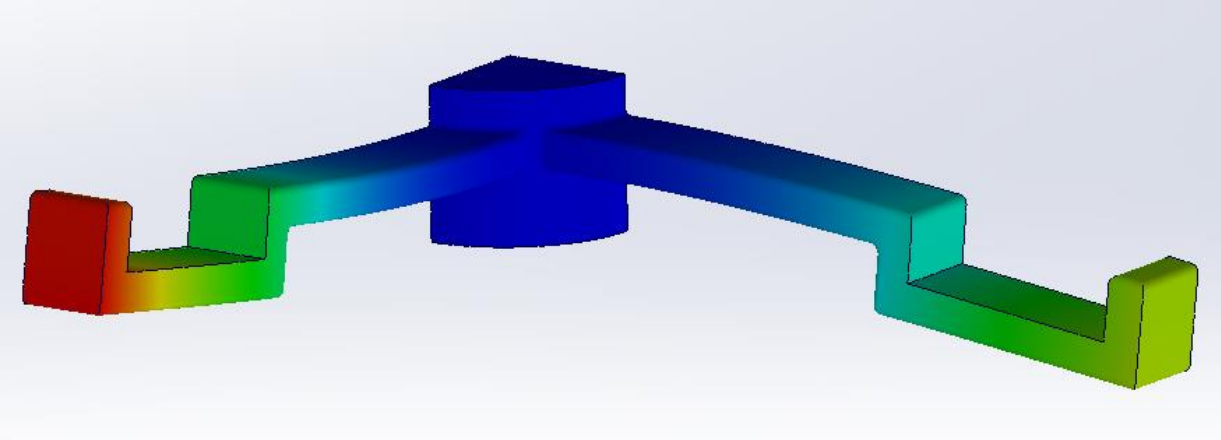

Figure 15: Mode shape at the fundamental natural frequency, Mesh Size: 0.1875mm

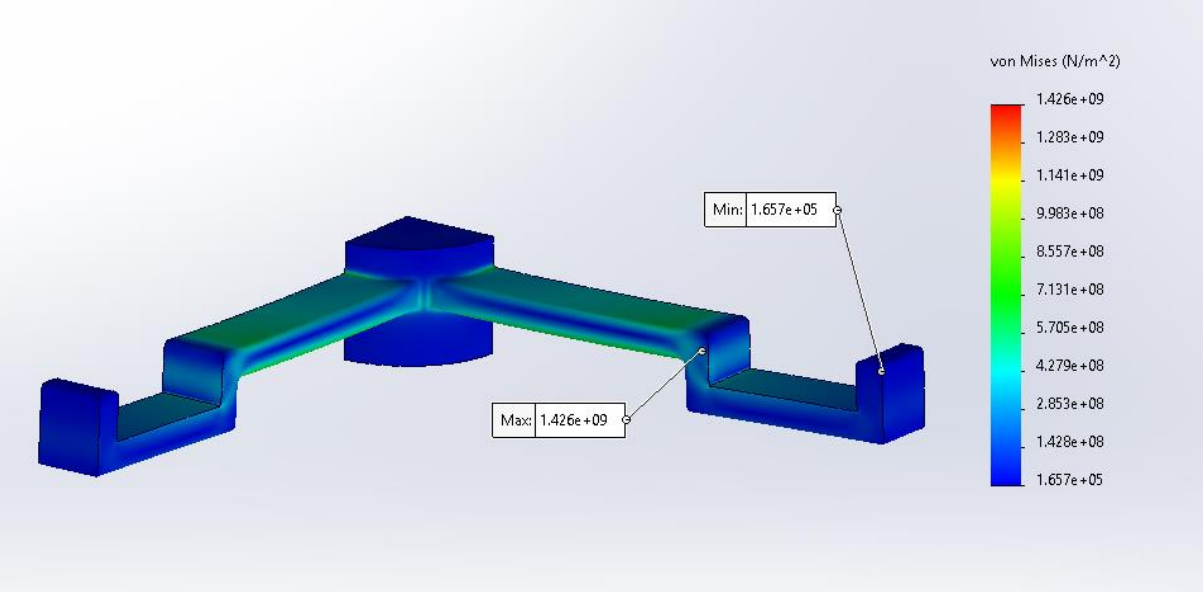

Figure 16: Von mises stress plot, Mesh Size: 0.1875mm

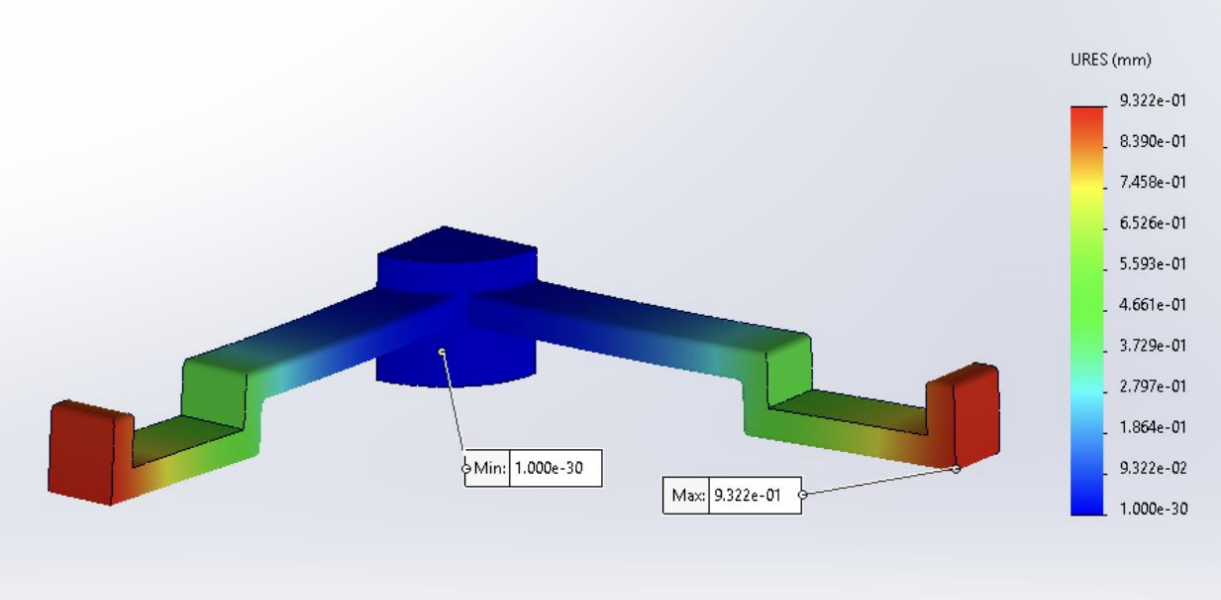

Figure 17: Total deformation plot, Mesh Size: 0.1875mm

Figures 14-17 demonstrate the locations of the maximum and minimum axial deflection (mm), total deflection (mm), Von Mises Stress (N/m^2), and the mode shape of the fundamental natural frequency (Hz). All images were generated using the final values denoted in Figure 11, and a mesh size of .1875mm.

Project Question Answers:

1. **Design the governor. Find the location of each leg on the shaft and the dimensions of each leg (find W, t, Ll, L2, and d).**

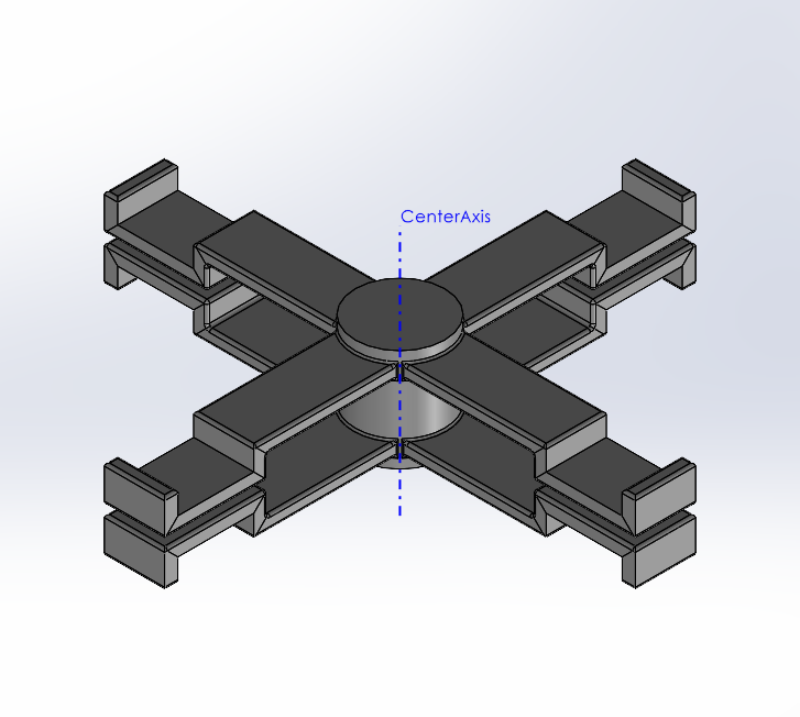

Figure 18: Final governor part render, containing 4 legs spanning 360 degrees with equal spacing.

The dimensions are as follows:

W = 6.75mm

t = 1.5mm

L1 = 14.75mm

L2 = 8.5mm

d = 1.5mm

2. **What is the maximum stress, and where does it occur?**

The maximum Von Mises (N/m^2) stress is 1421MPa, and it occurs on the underside of the first bend in the Governor arm. The location is shown in the figure below.

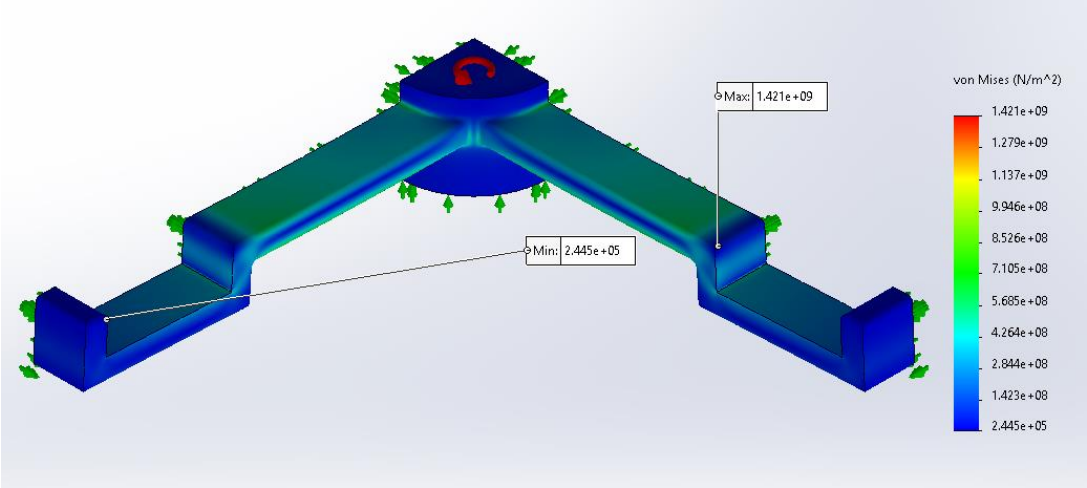

Figure 19: Von Mises stress plot with maximal and minimal values displayed, utilizing a mesh size of 0.6mm

3. **What is the maximum axial and total deformation?**

The maximum axial deformation is .9196mm in the Z-direction. The part was defined with Z-up instead of Y-up orientation. The total deformation is 1.421E+09 N/m^2, which is equivalent to 1421 MPa.

4. **Plot the governor's axial deflection vs. its angular velocity.**

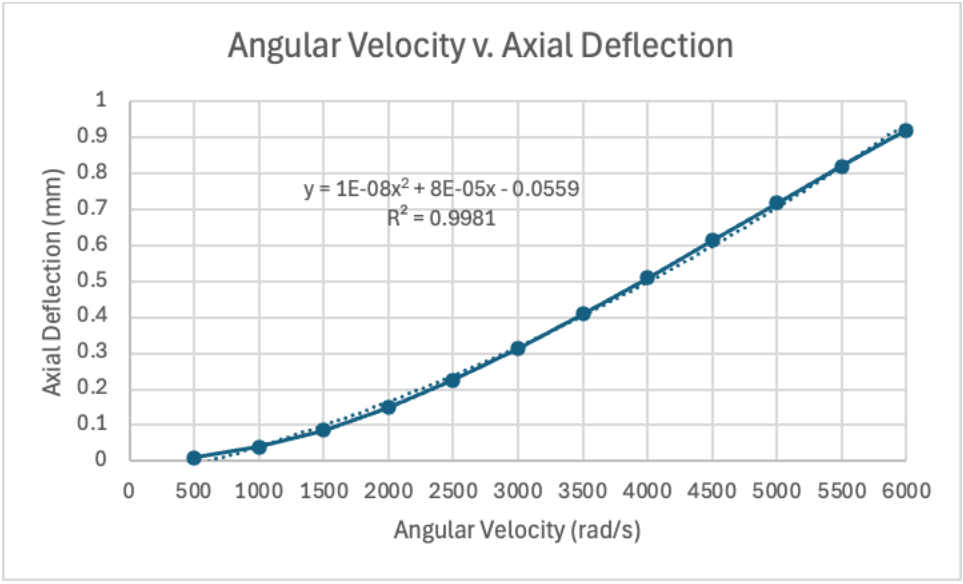

Figure 20: Plot of Angular Velocity vs Axial Deflection with an exponential trendline at 0.5mm mesh size

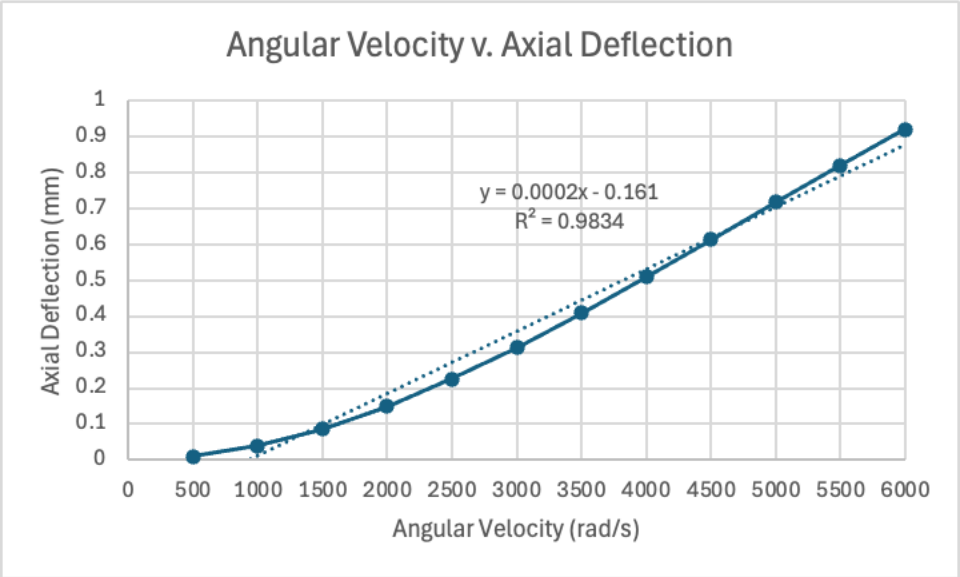

Figure 21: Plot of Angular Velocity vs Axial Deflection with a linear trendline at 0.5mm mesh size

5. What is the mass of the part?

The mass of the part is 3.267 grams.

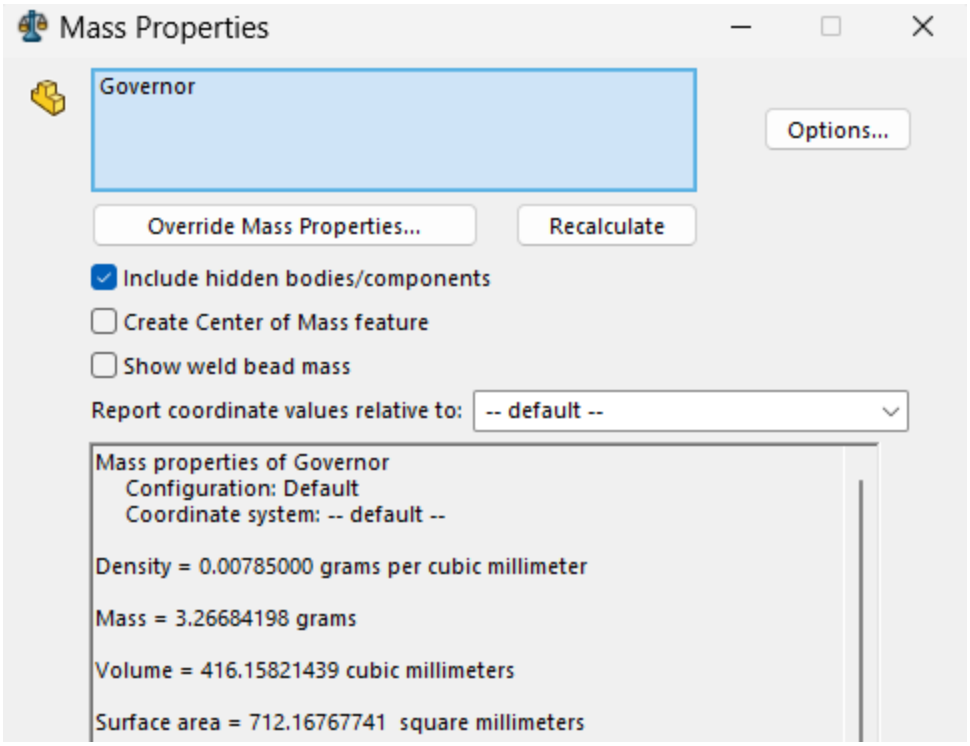

Figure 22: Mass properties table in SolidWorks

Final Values Table

Score	t (mm)	L1 (mm)	L2 (mm)	W (mm)	d (mm)
96.872619	1.5	14.75	8.5	6.75	1.5
1.4*L2 <= L1 <= 1.8*L2?	L1+L2+t<25mm?	<2000Hz?	<1.15mm?	In Container?	Fillets?
YES	YES	YES	YES	YES	YES
Total Length	δ_total (mm)	f1 (Hz)	δ_axial (mm)	Mass (g)	σ_max (MPa)
24.75	0.9324	1567.6	0.9196	3.266842	1421

Figure 23: Final values table with final design dimensions, stresses, deflections, frequency, and other related items

Summary and conclusion

This project involved the complete design, optimization, and structural validation of a centrifugal governor component subject to geometric, operational, and performance constraints. The design variables L_1, L_2, t, W, and d were restricted to multiples of 0.25 mm, and governed by specific proportional and dimensional relationships, including the requirement that $1.4L_2 \leq L_1 \leq 1.8L_2$, that $L_1 + L_2 + t < 25$ mm, and that $0.75 \text{ mm} \leq d \leq 2.0$ mm. Additional requirements established that the legs must be as wide as possible, the part should be optimized to be wide, long, and thin in that priority order, and that thickness must remain small relative to geometry. A final constraint was imposed during refinement, requiring $t \leq 0.5 \cdot d$, removing any combination in which thickness exceeded half the diameter. To compare and rank viable geometries, a scoring equation was developed and applied:

$$\text{Score} = 100(0.5 \cdot W\_norm + 0.3 \cdot L\_norm + 0.2 \cdot T\_norm),$$

which normalized and weighted width, length, and thinness based on design priority.

In summary, the part was designed per the project guidelines, and the optimal configuration was determined through a combination of requirement interpretation, FEA, trend analysis, optimization, and convergence studies. Constraint filtering and trend mapping reduced the millions of theoretical combinations to a small pool of viable solutions, and subsequent optimization and FEA evaluation narrowed the selection further until it was determined that critical dimensions were maximized without violating geometric, frequency, or deflection limits. During refinement, the maximum von Mises stress was successfully moved away from the critical intersection of the arms with the central shaft through the strategic application of targeted fillets—specifically a 0.2 mm fillet at the arm–shaft junction and a 0.3 mm fillet along the part—which redistributed stresses and significantly reduced concentration in that high-risk region.

Static and frequency analyses were performed using a reduced symmetry model to efficiently evaluate structural response while maintaining physical representativeness. A mesh convergence

study confirmed that stress, displacement, and modal frequency stabilized within acceptable bounds, validating confidence in the selected geometry. The final optimized configuration successfully satisfied all constraints by maximizing width, minimizing thickness, and achieving a total axial length near the allowable limit while maintaining axial deflection below the container clearance, limiting maximum stress, and ensuring the fundamental natural frequency remained below the 2000 Hz requirement.

Overall, this structured and iterative approach enabled the development of a reliable and optimized centrifugal governor design that balances performance, manufacturability, and geometric constraints. The combination of parametric modeling, trend-driven elimination, and simulation-based optimization proved effective in converging a solution supported both numerically and analytically. Future work may include tolerance-based sensitivity studies, further fillet optimization, or experimental validation, but within the scope of this assignment, the final design represents a successful and well-justified engineering solution to the stated problem.